Amino Acids (2015) 47:175–187
DOI 10.1007/s00726-014-1853-5

ORIGINAL ARTICLE

N-acyl-ω-aminoaldehydes are efficient substrates of plant aminoaldehyde dehydrogenases

Jan Frömmel · Marek Šebela · Gabriel Demo · René Lenobel · Tomáš Pospíšil · Miroslav Soural · David Kopečný

Received: 1 July 2014 / Accepted: 7 October 2014 / Published online: 26 October 2014

Abstract Plant aminoaldehyde dehydrogenases (AMADHs, EC 1.2.1.19) belong to the family 10 of aldehyde dehydrogenases and participate in the metabolism of compounds related to amino acids such as polyamines or osmoprotectants. Their broad specificity covers ω-aminoaldehydes, aliphatic and aromatic aldehydes as well as nitrogen-containing heterocyclic aldehydes. The substrate preference of plant AMADHs is determined by the presence of aspartic acid and aromatic residues in the substrate channel. In this work, 15 new *N*-acyl derivates of 3-aminopropanal (APAL) and 4-aminobutanal (ABAL) were synthesized and confirmed as substrates of two pea AMADH isoenzymes (PsAMADH 1 and 2). The compounds were designed considering the previously demonstrated conversion of *N*-acetyl derivatives as well as substrate channel dimensions (5–8 Å × 14 Å). The acyl chain length and its branching were found less significant for substrate properties than the length of the initial natural substrate. In general, APAL derivatives were found more efficient than the corresponding ABAL derivatives because of the prevailing higher conversion rates and lower K_m values. Differences in enzymatic performance between the two isoenzymes corresponded in part to their preferences to APAL to ABAL. The higher PsAMADH2 affinity to substrates correlated with more frequent occurrence of an excess substrate inhibition. Molecular docking indicated the possible auxiliary role of Tyr163, Ser295 and Gln451 in binding of the new substrates. The only derivative carrying a free carboxyl group (*N*-adipoyl APAL) was surprisingly better substrate than ABAL in PsAMADH2 reaction indicating that also negatively charged aldehydes might be good substrates for ALDH10 family.

Abbreviations for names of all new synthetic *N*-acyl-ω-aminoaldehydes (15 compounds) are completely elucidated in the supplementary file 1 (Met stands for methyl, Propi for propionyl, Butyr for butyryl, Valer for valeryl and Adip for adipoyl).

Electronic supplementary material The online version of this article (doi:10.1007/s00726-014-1853-5) contains supplementary material, which is available to authorized users.

J. Frömmel · M. Šebela (✉) · R. Lenobel · D. Kopečný (✉)
Department of Protein Biochemistry and Proteomics, Centre of the Region Haná for Biotechnological and Agricultural Research, Faculty of Science, Palacký University, Šlechtitelů 11, 783 71 Olomouc, Czech Republic
e-mail: marek.sebela@upol.cz

D. Kopečný
e-mail: kopecny_david@yahoo.co.uk

G. Demo
Central European Institute of Technology, Masaryk University, Kamenice 5, 625 00 Brno, Czech Republic

G. Demo
National Centre for Biomolecular Research, Faculty of Science, Masaryk University, Kamenice 5, 625 00 Brno, Czech Republic

T. Pospíšil
Department of Chemical Biology, Centre of the Region Haná for Biotechnological and Agricultural Research, Faculty of Science, Palacký University, Šlechtitelů 11, 783 71 Olomouc, Czech Republic

M. Soural
Department of Organic Chemistry, Faculty of Science, Palacký University, 17. listopadu 12, Olomouc CZ-771 46, Czech Republic

M. Soural
Institute of Molecular and Translational Medicine, Faculty of Medicine and Dentistry, Palacký University, Hněvotínská 5, Olomouc CZ-779 00, Czech Republic

Keywords *N*-acylation · Aminoaldehyde dehydrogenase · Isoenzyme · KF-celite · NAD^+ · Substrate docking

Abbreviations

Ac-ABAL	4-Acetamidobutanal
Ac-APAL	3-Acetamidopropanal
ALDH	Aldehyde dehydrogenase
AMADH	Aminoaldehyde dehydrogenase
APAL	3-Aminopropanal
ABAL	4-Aminobutanal
BAL	Betaine aldehyde
BADH	Betaine aldehyde dehydrogenase
GABA	4-Aminobutyric acid
GBAL	4-Guanidinobutanal
PsAMADH	Aminoaldehyde dehydrogenase from pea (*Pisum sativum*)
TMABAL	4-Trimethylaminobutanal

Introduction

Aldehyde dehydrogenases (ALDHs) constitute a superfamily of oxidoreductive enzymes. ALDH10 family members in plants are aminoaldehyde dehydrogenases (AMADHs) and oxidize ω-aminoaldehydes to the corresponding amino acids using $NAD(P)^+$ as a coenzyme (Brocker et al. 2013). Because of their broad substrate specificity, the enzymes used to be named 4-aminobutyraldehyde dehydrogenases (ABALDHs, EC 1.2.1.19), 4-guanidinobutyraldehyde dehydrogenases (GBALDHs, EC 1.2.1.54) and betaine aldehyde dehydrogenases (BADHs, EC 1.2.1.8). There are several crystal structures of plant ALDH10 enzymes available (Tylichová et al. 2010; Díaz-Sánchez et al. 2012; Kopečný et al. 2013). The enzymes exist as homodimers with a typical ALDH subunit fold comprising a catalytic domain, a coenzyme-binding domain and an oligomerization domain. There is also a 14-Å-long substrate channel in each monomer. The active site contains three strictly conserved residues (Asn, Glu and Cys) that are essential for the catalysis. Usually, there are two isoforms in plants with different substrate specificity. PsAMADH1 and PsAMADH2 in pea (*Pisum sativum*) differ in a few substrate-channel residues: Ala109/Trp109, Phe288/Trp288 and Ser453/Cys453, respectively (Tylichová et al. 2010). ALDHs of the family 10 participate in several metabolic pathways: polyamine catabolism, production of osmoprotectants and carnithine biosynthesis (Díaz-Sánchez et al. 2012; Kopečný et al. 2013).

Natural substrates of plant AMADHs include for example 3-aminopropanal (APAL) (Awal et al. 1995), 4-aminobutanal (ABAL), 4-guanidinobutanal (GBAL) (Matsuda and Suzuki 1984), 4-trimethylaminobutanal (TMABAL) (Fujiwara et al. 2008) or betaine aldehyde (BAL) (Weigel et al. 1986). Polyamine-derived APAL is reactive and cytoxic. Thus, its oxidation to β-alanine represents a detoxification process (Li et al. 2003). ABAL arises from putrescine oxidation by diamine oxidase (EC 1.4.3.22) and spontaneously cyclizes to non-toxic 1-pyrroline (Smith et al. 1986). ABAL or 1-pyrroline oxidation provides 4-aminobutyric acid (GABA) (Shelp et al. 2012). On the other hand, a lack of ABAL oxidation leads to the production of 2-acetyl-1-pyrroline in aromatic rice varieties (Bradbury et al. 2008). GBAL originates from arginine degradation (Matsuda and Suzuki 1984) and its oxidation produces 4-guanidinobutyric acid.

BAL is produced by choline oxidation and finally converted by ALDH10 enzymes specific for this compound (frequently referred to as BADHs) to glycine betaine (betaine), a compatible osmolyte protecting against drought and salinity (Rhodes et al. 1989). The acetylated polyamines N^1-acetylspermine and N^1-acetylspermidine are oxidized by N^1-acetylpolyamine oxidase (EC 1.5.3.13) to spermidine and putrescine (Tavladoraki et al. 2006), respectively, and 3-acetamidopropanal (Ac-APAL), which is another natural substrate of plant AMADHs (Kopečný et al. 2013). Aliphatic aldehydes are only weak substrates (Tylichová et al. 2010).

Plant AMADHs also oxidize a wide range of synthetic aromatic aldehydes containing benzene, pyridine, pyrimidine or purine ring (Frömmel et al. 2012). These compounds are typically metabolized by other members of the ALDH superfamily such as nonspecific ALDHs (EC 1.2.1.3) (Peng et al. 2005), benzaldehyde dehydrogenase (1.2.1.28) (Gaid et al. 2009; Long et al. 2009) or *p*-hydroxybenzaldehyde dehydrogenase (EC 1.2.1.64) (Chakraborty et al. 2009). Substrate properties of aromatic aldehydes are influenced by the position of a possible substituent, when a higher distance from the aldehyde group is more favorable (Frömmel et al. 2012).

The carboxylic acids produced by AMADH reaction in plants can be further metabolized. For example, β-alanine can be methylated to yield the osmoprotectant β-alanine betaine (Hanson et al. 1994). GABA is incorporated into the citric acid cycle after its transamination and oxidation to succinic acid (Shelp et al. 1999). The oxidation of TMABAL (derived from lysine) in plants probably represents a step in the biosynthesis of carnitine (Rippa et al. 2012), which is used for fatty acid transportation in the mitochondrion, as it is well known in mammals (Vaz and Wanders 2002). Glycine betaine is not further metabolized as has been demonstrated in sugar beet and its wild progenitor (Hanson and Wyse 1982). No radioactive metabolites of [^{14}C] glycine betaine were detected in these plants upon feeding experiments.

Based on the fact that Ac-APAL is an efficient substrate of plant ALDH10 enzymes (Kopečný et al. 2013) and also

4-acetamidobutanal (Ac-ABAL) is well oxidized by certain representatives of this group (Bradbury et al. 2008), it was challenging to evaluate substrate properties of a series of *N*-acyl-ω-aminoaldehydes with a different length and branching of the acyl chain. A total of 15 new compounds were synthesized and subjected to oxidation by PsAMADH1 and PsAMADH2. They were all found substrates.

Materials and methods

Chemicals

Diethylacetals of APAL and ABAL as well as NAD^+ were from Sigma-Aldrich Chemie (Steinheim, Germany). The following acyl chlorides were purchased from the same vendor: acetyl chloride, butyryl chloride, isobutyryl chloride, isovaleryl chloride, methyl adipoyl chloride, 2-methyl butyryl chloride, propionyl chloride, valeryl chloride and trimethylacetyl chloride. All other chemicals were of analytical purity grade.

Preparation of enzymes

PsAMADH1 and PsAMADH2 were used as recombinant proteins. The procedure of cloning, expression and purification of both enzymes was described earlier (Tylichová et al. 2008, 2010). Protein concentration was assayed by a colorimetric method with bicinchoninic acid (Smith et al. 1985) or by a direct measurement at 280 nm on a BioSpec-nano micro-volume spectrophotometer (Shimadzu, Kyoto, Japan) using calculated extinction coefficients (Tylichová et al. 2010).

Synthesis of N-acyl-ω-aminoaldehydes

Diethylacetals of APAL and ABAL were subjected to *N*-acylation with acyl chlorides using KF-Celite as a heterogeneous catalyst (Ando and Yamawaki 1979). KF-Celite (5 g) was suspended in acetonitrile (50 ml; dried by sodium sulfate) containing APAL or ABAL diethylacetal (6 mmol) and the mixture was kept at laboratory temperature under continuous stirring on a magnetic stirrer. After 15 min of stirring, an acylchloride (6 mmol) was added dropwise over a period of 30 min. Then the resulting solution was set aside for another 30 min. Later on, KF-Celite was filtered out and acetonitrile removed from the filtrate in a rotary vacuum evaporator. Acetyl derivatives of APAL and ABAL were prepared according to previous protocols (Wood et al. 2007; Kopečný et al. 2013).

Routine NMR spectra for purity evaluation of the synthesized compounds were acquired on a JEOL JNM-ECA 500 (JEOL, Tokyo, Japan; ^{1}H, 500 MHz; ^{13}C, 125 MHz) spectrometer equipped with a 5 mm JEOL Royal probe. Data analysis was performed in DELTA NMR software (JEOL). ^{1}H NMR and ^{13}C NMR chemical shifts (δ) were calibrated using tetramethylsilane (TMS, ^{1}H $\delta = 0$ ppm) or solvents: $CDCl_3$ (^{1}H $\delta = 7.25$ ppm, ^{13}C $\delta = 77.16$ ppm) or DMSO-d_6 (^{1}H $\delta = 2.46$ ppm, ^{13}C $\delta = 40.00$ ppm). The deuterated solvents were from Sigma-Aldrich Chemie.

Prior to activity assay, the synthesized acetals were converted to free aldehydes by 0.1 M hydrochloric acid after heating at 100 °C (Trossat et al. 1997). During such a treatment, diethylacetal of methyl-esterified *N*-adipoyl derivative of APAL was converted to a free *N*-adipoyl APAL because of the concomitant hydrolysis of the ester group.

Activity assay

AMADH activity was assayed by monitoring the production of NADH during oxidation of a substrate ($\varepsilon_{340} = 6{,}620$ l mol^{-1} cm^{-1}) as decribed (Tylichová et al. 2010). All measurements were performed on an Agilent 8453 UV–visible spectrophotometer (Agilent Technologies, Santa Clara, CA, USA) at 30 °C. The reaction mixture in a total volume of 2.0 ml contained 0.1 mol l^{-1} Tris–HCl, pH 9.0, 0.5 mmol l^{-1} NAD^+ and a proper amount of the enzyme (at the level of micrograms). The reaction was initiated by adding substrate: final concentrations of 1 mmol l^{-1} were chosen for evaluation of relative reaction rates. In experiments designed to obtain the steady-state kinetic parameters (K_m and V_{max}), the final concentration of substrate usually varied between 0.05–4 mmol l^{-1} and 0.02–2 mmol l^{-1} for PsAMADH1 and PsAMADH2 reaction, respectively. All kinetic measurements were carried out in triplicates. Data analysis was performed with GraphPad Prism 5.0 software (GraphPad Software, La Jolla, CA, USA). The nonlinear regression used was based either on the Michaelis–Menten equation $v = V_{max}\cdot[S]/(K_m + [S])$ for common substrates or on a modified equation $v = V_{max}\cdot[S]/(K_m + [S]\cdot(1 + [S]/K_{ss}))$ for substrates showing excess substrate inhibition. In these equations, K_m denotes Michaelis constant, K_{ss} substrate inhibition constant, V_{max} maximum velocity, v initial velocity and [S] substrate concentration.

Detection of reaction products

In order to identify *N*-acylated amino acid products generated from the synthesized compounds, AMADH reaction mixtures were subjected to mass spectrometric analysis. At the beginning, PsAMADH2 (2.9 mg ml^{-1}) was dialyzed against 50 mM ammonium bicarbonate buffer, pH 8.0, at 4 °C overnight. Then the reaction mixture in a total volume of 4 ml contained 3.72 ml of 0.1 M ammonium bicarbonate, pH 8.0, 150 µl of 40 mM NAD^+, *N*-acyl-ω-aminoaldehyde

in a final concentration of 1.0 mM and 30 µl of the dialyzed enzyme solution. The reaction was started by substrate addition and proceeded on a magnetic stirrer at laboratory temperature overnight. The enzyme was removed by ultrafiltration using centrifugal filter units Amicon Ultra-0.5 with a cut-off of 10 kDa (Sigma-Aldrich Chemie). The ultrafiltrates were analyzed using a UHR-Q-TOF mass spectrometer maXis (Bruker Daltonik, Bremen. Germany) in the positive mode. Prior to analysis, the filtrate was diluted 10 times with water (MS quality, Sigma-Aldrich) and introduced by a syringe via syringe pump (Harward Apparatus, USA) into the ESI ion source at a flow rate of 3 µl min^{-1}. The MS parameter settings were as follows: capillary source, 4,500 V; dry gas, 4 l min^{-1}; desolvatation gas, 0.6 bar; dry temperature, 180 °C. Tune page settings were optimized for an acquisition of a low-molecular-weight compound. MS spectra were recorded in the mass range of *m/z* 50–500 with a frequency of 1 Hz.

Substrate docking into the crystal structures

To better understand their interaction with PsAMADHs, the synthesized acylaminoaldehydes as well as two physiological substrates APAL and ABAL were docked into the active site of PsAMADH2 (PDB code 3IWJ). The procedures of working with the protein structure were done in the same way as described for docking of dichloropyridine carbaldehydes and pyridinyl methyl aminoaldehydes into the active site of PsAMADH2 (Frömmel et al. 2012). All ligand structures were built by PRODRG server (Schüttelkopf and van Aalten 2004; http://www.davapc1.bioch.dundee.ac.uk/cgi-bin/prodrg). The geometries of the ligand structures were optimized using the Hartree–Fock method with a 6-31G* basis set as implemented in the Gaussian 03 program (Frisch et al. 2004). The electro-static potential fitting (ESP) charges were calculated, and the RESP procedure of the Antechamber program from the AMBER suite was used to generate input files for docking programs (Case et al. 2005; Pearlman et al. 1995). The graphical user interface software Triton (Prokop et al. 2008) was employed to prepare, run, and analyze the docking simulations. Autodock 3.0 was used as a molecular docking tool (Morris et al. 1998) following the semi-flexible docking protocol with rigid target PsAMADH2 protein and flexible ligands (all rotatable dihedrals with exception of the aldehyde were allowed to rotate freely). Grid maps calculation was performed by AutoGrid 3.0 using the grid box (45 × 45 × 45 Å) centered to the substrate channel. Lamarckian genetic algorithm was used to accomplish docking calculations and a maximum of 200 conformers was considered for each compound. The population size was set to 50 and the individuals were initialized randomly. The maximum number of energy evaluations was 5×10^6 with the cluster tolerance 0.5 Å. Images of the most probable aldehyde position at the active site of PsAMADH2 were drawn by the PyMOL molecular graphic system, version 1.3 (Schrödinger LLC, USA; http://www.pymol.org).

Results and discussion

In this work, a series of new derivatives of two natural substrates of plant AMADHs, namely APAL and ABAL, was synthesized using *N*-acylation reactions with carboxylic acid chlorides as modifiers of the ω-amino group. The compounds were designed based on the shape of the substrate channel of the enzymes, which is 14 Å long and 5-8 Å wide (Tylichová et al. 2010). The middle-section diameter size of the channel is related to substrate specificity (Kopečný et al. 2013). It was therefore expected that

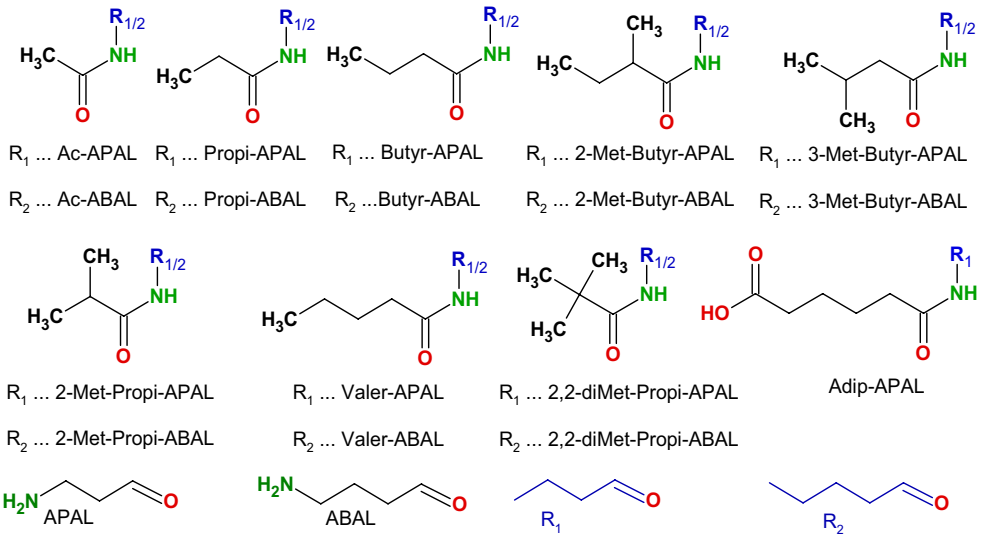

Fig. 1 An overview of synthetic *N*-acyl-ω-aminoaldehydes. Molecular formulas of the analyzed compounds were drawn by ChemSketch 2.0 software (Advanced Chemistry Development, Toronto, Canada)

the presence of short acyl chains (up to five carbon atoms) at the amino group of a natural aminoaldehyde substrate would not prevent from its oxidation. On the other hand, a certain degree of variability in substrate efficiency resulting from the length and branching of the acyl group was assumed. Chemical syntheses involved diethylacetals of APAL and ABAL as starting compounds and Celite coated with potassium fluoride (KF-Celite) as a heterogeneous catalyst (Ando and Yamawaki 1979). All products were worked-up by removing the solvent on a rotary vacuum evaporator and obtained in a high yield (above 80 %). Chemical formulas of newly synthesized compounds as well as those of the respective acetyl derivatives are shown in Fig. 1. Purity of the products was checked and confirmed by NMR spectrometry. ^{1}H- and ^{13}C-NMR spectral data are available as supplementary file 1, where also abbreviations for names of the compounds are elucidated.

Substrate properties of all synthetic compounds were studied by kinetic measurements with two pea isoenzymes PsAMADH1 and PsAMADH2. Enzyme activity was analyzed on a spectrophotometer by monitoring the reduction of the coenzyme NAD^{+} at 340 nm. The relative reaction rates at a substrate concentration of 1.0 mmol l^{-1} were in the range of 25–95 % for PsAMADH1 and 18–141 % for PsAMADH2 when compared with that of APAL oxidation (arbitrarily taken as 100 %). A similar comparison with respect to the ABAL oxidation rate showed the following values: 29–108 % and 55–433 %, respectively (supplementary file 2). These data allowed setting up further experiments and recognizing certain rules with respect to the contribution of the acyl chain length and the presence of C3 or C4 core aminoaldehyde on substrate efficiency. The concentration of substrates used (1 mmol l^{-1}) is much higher than the K_m values for APAL and ABAL (~10^{-5} mol l^{-1}; Tylichová et al. 2010) and hence it can be expected that the enzymes would perform optimally in the cell at such a level of physiological or exogenous substrates. Generally, both isoenzymes oxidized *N*-acylated APAL derivatives more readily than the corresponding ABAL derivatives according to this rough evaluation (with an exception of 2,2-diMet-Propi-ABAL versus 2,2-diMet-Propi-APAL in the reaction of PsAMADH1). The relative reaction rates for the oxidation of ABAL derivatives calculated towards the ABAL conversion rate were similar to the relative reaction rates for APAL derivatives carrying the same acyl chain calculated towards the APAL conversion rate. Thus, the

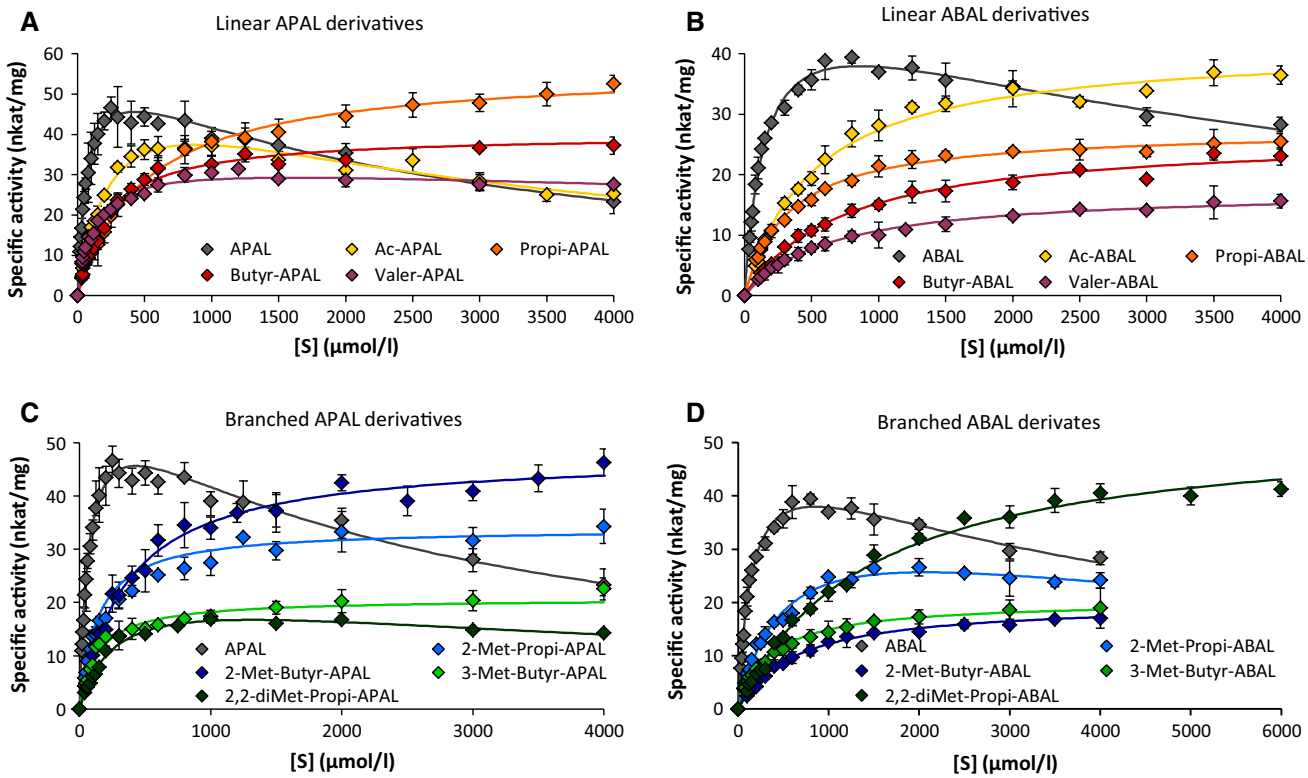

Fig. 2 Saturation curves of PsAMADH1 reactions with *N*-acyl-ω-aminoaldehydes. *Black curves* were chosen for the physiological substrates APAL and ABAL. Saturation curves of their linear derivatives are drawn in *yellow*, *orange*, *magenta* and *red* and those of branched derivatives in shades of *blue* and *green*. **a** Oxidation of linear *N*-acyl derivatives of APAL by PsAMADH1; **b** oxidation of linear *N*-acyl derivatives of ABAL by PsAMADH1; **c** oxidation of branched *N*-acyl derivatives of APAL by PsAMADH1; **d** oxidation of branched *N*-acyl derivatives of ABAL by PsAMADH1. See "Materials and methods" for experimental details

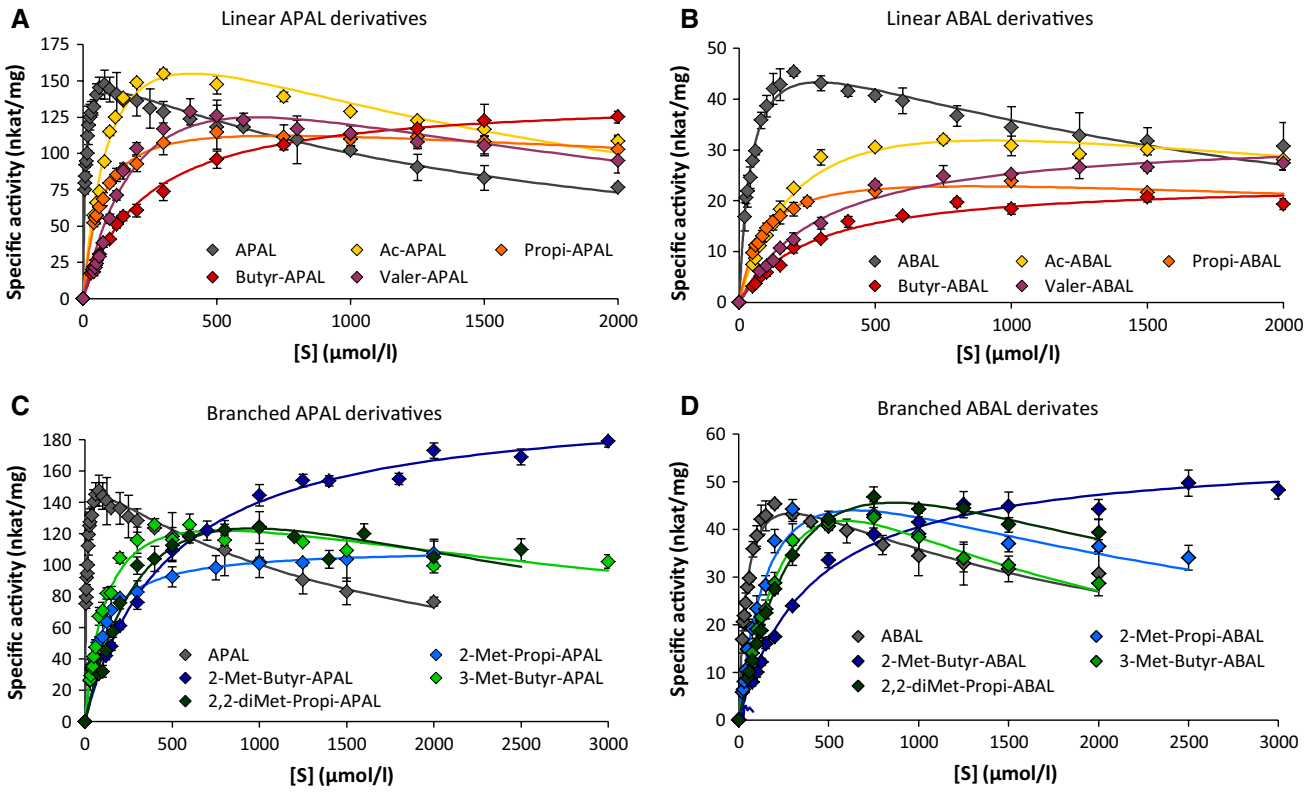

Fig. 3 Saturation curves of PsAMADH2 reactions with *N*-acyl-ω-aminoaldehydes. *Black curves* were chosen for the physiological substrates APAL and ABAL. *Saturation curves* of their linear derivatives are drawn in *yellow*, *orange*, *magenta* and *red* and those of branched derivatives in shades of *blue* and *green*. **a** Oxidation of linear *N*-acyl derivatives of APAL by PsAMADH2, **b** oxidation of linear *N*-acyl derivatives of ABAL by PsAMADH2; **c** oxidation of branched *N*-acyl derivatives of APAL by PsAMADH2; **d** oxidation of branched *N*-acyl derivatives of ABAL by PsAMADH2. See "Materials and methods" for experimental details

proportional factor for the same type of derivative appeared to be more or less constant. In the case of substrate conversion by PsAMADH1, APAL or ABAL derivatives with an unbranched acyl chain were converted at rates decreasing with the length of the chain. Interestingly, the same substrates did not fully display such a feature when oxidized by PsAMADH2.

It has been shown for ALDHs from the family 3 in *Arabidopsis thaliana* that the NAD^+ or $NADP^+$ coenzyme saturation concentrations vary depending on the aldehyde substrate. For example, in the case of ALDH3H1, the K_m value for NAD^+ was 3.5 times higher in the presence of hexanal than using nonenal as a substrate (Stiti et al. 2011). As regards to PsAMADH, such a behavior has not been reported. The K_m values of PsAMADH1 and PsAMADH2 for NAD^+ determined in the presence of APAL as a substrate are 40 and 55 µmol l^{-1}, respectively (Tylichová et al. 2010). Using ABAL as a substrate, both values appear around 50 µmol l^{-1} (Frömmel, unpublished results). The affinity of PsAMADH1 and 2 to the coenzyme NAD^+ did not change markedly in the presence of the synthetic substrates. The kinetic data obtained with variable NAD^+ concentrations and representative branched or unbranched *N*-acyl-ω-aminoaldehydes (at a fixed concentration of 1 mmol l^{-1}) are shown in supplementary file 3. In all cases, the K_m value for NAD^+ of 10–70 µM was determined.

Figures 2 and 3 provide an overview of saturation curves obtained from kinetic experiments at different substrate concentrations. The values of Michaelis constant of PsAMADH1 and PsAMADH2 for the synthetic substrates were in the range of 120–1,420 and 39–531 µmol l^{-1}, respectively, when subtracted from nonlinear regression of the corresponding curves (Table 1). The K_m values of PsAMADH1 for the *N*-acyl-ω-aminoaldehydes were at least two times higher than those for the natural substrates APAL and ABAL. Surprisingly, PsAMADH2 showed in some cases much higher differences such as 10 fold or even 60 fold. With only a few exceptions (Valer-APAL, 2-Met-Butyr-APAL and 3-Met-Butyr-ABAL), PsAMADH2 showed higher affinity to the newly synthesized compounds than PsAMADH1. Although the K_m value of PsAMADH2 for 3-Met-Butyr-APAL was almost the same as that for PsAMADH1, it increased (up to 160 µmol l^{-1}) after omitting

Table 1 Kinetic parameters of oxidation of *N*-acyl-ω-aminoaldehydes by PsAMADH1 and PsAMADH2

Substrate	Kinetic parameters			
	PsAMADH1		PsAMADH2	
	K_m (μmol l^{-1})	k_{cat} (s^{-1})	K_m (μmol l^{-1})	k_{cat} (s^{-1})
Reference substrates				
APAL	71.8 ± 5.75	3.65 ± 0.122	7.27 ± 0.46	9.42 ± 0.146
ABAL	153 ± 15.4	3.10 ± 0.151	45.9 ± 6.86	3.02 ± 0.147
Synthetic substrates				
Ac-APAL	268 ± 31.3	3.61 ± 0.227	109 ± 21.7	13.9 ± 1.34
Propi-APAL	492 ± 23.3	3.40 ± 0.049	65.1 ± 3.77	7.72 ± 0.170
Butyr-APAL	227 ± 32.1	2.41 ± 0.072	226 ± 9.5	8.13 ± 0.111
2-Met-Propi-APAL	183 ± 18.0	2.03 ± 0.061	93.5 ± 2.66	6.49 ± 0.053
Valer-APAL	120 ± 11.2	2.02 ± 0.070	271 ± 66.8	11.0 ± 1.56
2-Met-Butyr-APAL	366 ± 40.6	2.87 ± 0.092	469 ± 33.1	12.1 ± 0.27
3-Met-Butyr-APAL	137 ± 19.9	1.24 ± 0.046	130 ± 17.0	9.54 ± 0.544
2,2-DiMet-Propi-APAL	266 ± 31.7	1.41 ± 0.085	477 ± 130.0	14.4 ± 2.47
Adip-APAL	431 ± 39.3	1.03 ± 0.053	39.2 ± 3.99	8.78 ± 0.305
Ac-ABAL	516 ± 41.0	2.49 ± 0.070	242 ± 33.4	2.84 ± 0.209
Propi-ABAL	327 ± 14.0	1.65 ± 0.019	92.7 ± 7.69	1.63 ± 0.060
Butyr-ABAL	738 ± 60.0	1.60 ± 0.005	264 ± 34.7	1.39 ± 0.056
2-Met-Propi-ABAL	525 ± 65.3	2.32 ± 0.016	189 ± 33.9	4.08 ± 0.397
Valer-ABAL	629 ± 35.1	1.05 ± 0.020	304 ± 39.0	1.93 ± 0.070
2-Met-Butyr-ABAL	638 ± 24.8	1.20 ± 0.014	397 ± 43.3	1.56 ± 0.128
3-Met-Butyr-ABAL	361 ± 18.1	1.22 ± 0.020	531 ± 113.7	6.84 ± 1.088
2,2-diMet-Propi-ABAL	1,420 ± 94	3.20 ± 0.083	506 ± 73.7	5.80 ± 0.595

Enzyme activity with substrates at varying final concentrations was measured in 0.1 mol l^{-1} Tris–HCl buffer, pH 9.0, at 30 °C

NAD^+ concentration in the reaction mixture was 0.5 mmol l^{-1}

The GraphPad Prism 5.0 software was used to calculate K_m and V_{max} values, k_{cat} comes from V_{max} divided by concentration of enzyme active sites

data obtained for high substrate concentrations (where an excess substrate inhibition was observed—see further). The K_m values for Butyr-APAL conversion by both isoenzymes were found the same based on the nonlinear regression (Table 1). In most cases, the K_m values for APAL derivatives were found lower than those for the corresponding ABAL derivates. There were only two exceptions: Propi-APAL/Propi-ABAL in PsAMADH1 reaction and 2-Met-Butyr-APAL/2-Met-Butyr-ABAL in PsAMADH2 reaction. For PsAMADH2, the Michaelis constant rather increased with the length of the acyl chain of C3–C5 unbranched substrates. This was not the case for PsAMADH1 and APAL derivatives: here the K_m value for Propi-APAL was higher than those for Butyr-APAL and Valer-APAL. Nevertheless, in three of four possibilities, the K_m values for Propi-APAL or Propi-ABAL were the lowest among all substrates comprising an unbranched C3–C5 acyl chain at the amino group. The K_m value of PsAMADH1 for Adip-APAL was higher than those for other APAL derivatives except for Propi-APAL. Interestingly, in the case of PsAMADH2 reaction, the K_m value for Adip-APAL was the lowest one from all synthetic compounds.

The effect of branching of the acyl chain was as follows: (1) the K_m values for Val-APAL and Val-ABAL were lower than those for the corresponding *N*-(2-methylbutyryl)aminoaldehydes; (2) the K_m values for 3-Met-Butyr-APAL and 3-Met-Butyr-ABAL were usually lower than those for the corresponding *N*-(2,2-dimethylpropionyl)aminoaldehydes; (3) the K_m values for Butyr-APAL and Butyr-ABAL were higher than those for the corresponding *N*-(2-methylpropionyl)aminoaldehydes; (4) the aminoaldehydes with 2-methylpropionyl chain were accepted by both isoenzymes with higher affinity than those with 2-methylbutyryl chain; (5) although the affinity of PsAMADH2 to *N*-(2-methylpropionyl)aminoaldehydes was higher than to *N*-(3-methylbutyryl)aminoaldehydes, an inverted result was achieved for PsAMADH1.

The V_{max} values determined for the synthetic derivatives reflected enzyme activities measured with the original compounds APAL and ABAL. When mutually compared,

Table 2 Catalytic efficiency of PsAMADH1 and PsAMADH2 for *N*-acyl-ω-aminoaldehydes

Substrate	Catalytic efficiency			
	Absolute [k_{cat}/K_m (mol^{-1} l s^{-1})]		Relative [$(k_{cat}/K_m)_{substrate}/(k_{cat}/K_m)_{APAL}$]	
	PsAMADH1	PsAMADH2	PsAMADH1	PsAMADH2
Reference substrates				
APAL	5.09×10^4	1.30×10^6	1.000	1.000
ABAL	2.02×10^4	6.58×10^4	0.397	0.051
Synthetic substrates				
Ac-APAL	1.35×10^4	1.28×10^5	0.265	0.098
Propi-APAL	6.90×10^3	1.19×10^5	0.136	0.092
Butyr-APAL	1.06×10^4	3.60×10^4	0.208	0.028
2-Met-Propi-APAL	1.11×10^4	6.94×10^4	0.218	0.053
Valer-APAL	1.68×10^4	4.06×10^4	0.330	0.031
2-Met-Butyr-APAL	7.84×10^3	2.57×10^4	0.154	0.020
3-Met-Butyr-APAL	9.07×10^3	7.33×10^4	0.178	0.056
2,2-DiMet-Propi-APAL	5.30×10^3	3.02×10^4	0.104	0.023
Adip-APAL	2.39×10^3	2.24×10^5	0.047	0.172
Ac-ABAL	4.83×10^3	1.17×10^4	0.095	0.009
Propi-ABAL	5.05×10^3	1.75×10^4	0.099	0.013
Butyr-ABAL	2.16×10^3	5.27×10^3	0.042	0.004
2-Met-Propi-ABAL	4.42×10^3	2.16×10^4	0.087	0.017
Valer-ABAL	1.67×10^3	6.35×10^3	0.033	0.005
2-Met-Butyr-ABAL	1.88×10^3	3.92×10^3	0.037	0.003
3-Met-Butyr-ABAL	3.37×10^3	1.29×10^4	0.066	0.010
2,2-DiMet-Propi-ABAL	2.25×10^3	1.15×10^4	0.044	0.009

First, catalytic efficiency (k_{cat}/K_m) values of PsAMADH1 and PsAMADH2 for the oxidation of the synthesized *N*-acyl-ω-aminoaldehyde compounds were calculated based on the kinetic parameters presented in Table 1. Then, for calculating relative catalytic efficiency, the k_{cat}/K_m value for the reference substrate APAL was arbitrarily set at 1.000

in most cases they were higher for APAL derivatives than for the corresponding ABAL derivatives and the differences were much more pronounced for PsAMADH2 (not shown). Table 1 contains a list of k_{cat} values calculated from the respective V_{max} values when taking the dimeric character of the isoenzymes into consideration. All catalytic constants appeared between 1.0–3.6 s^{-1} for PsAMADH1 and 1.4–13.9 s^{-1} for PsAMADH2. Interestingly, in the case of PsAMADH2, all APAL derivatives were converted with k_{cat} values similar (>70 %) or even higher (five compounds) than those for reference substrate APAL. This was not observed for PsAMADH1 and probably represents a reflection of the more pronounced preference to APAL over ABAL of PsAMADH2 (Tylichová et al. 2010).

The catalytic efficiency values (k_{cat}/K_m) of PsAMADH1 and PsAMADH2 were calculated to sort the synthesized compounds objectively according to their substrate properties. They were at the level of 10^3–10^5 mol^{-1} l s^{-1} (Table 2). To obtain relative numbers for an easier comparison, the catalytic efficiency for APAL conversion was arbitrarily set at a value of 1.000 and the other values were recalculated accordingly. Then the relative catalytic efficiency values of PsAMADH1 and PsAMADH2 with *N*-acyl-ω-aminoaldehydes appeared in the range of 0.033–0.330 and 0.003–0.172, respectively (Table 2). In the given order, Valer-APAL, Ac-APAL and 2-Met-Propi-APAL were found the best three substrates of PsAMADH1 from the group of APAL derivatives, whereas Propi-ABAL, Ac-ABAL and 2-Met-Propi-ABAL were the best ones from the group of ABAL derivatives. In the case of PsAMADH2, such winners were Adip-APAL, Ac-APAL and Propi-APAL plus 2-Met-Propi-ABAL, Propi-ABAL and 3-Met-Butyr-ABAL, respectively. The k_{cat}/K_m value for Adip-APAL was almost two times higher than those for the second and third best substrates of PsAMADH2. Interestingly, Adip-APAL was three times better substrate of PsAMADH2 than ABAL (Table 2). No strict correlation was found between the catalytic efficiency values and the acyl chain length of the substrate. As regards to unbranched derivatives, acetyl and propionyl compounds were in most cases better substrates than butyryl and valeryl compounds (with an exception of APAL derivatives oxidized by PsAMADH1).

Table 3 Excess substrate inhibition observed in PsAMADH1 and PsAMADH2 reactions

Substrate	Substrate inhibition constants	
	PsAMADH1 [K_{ss} (μmol l^{-1})]	PsAMADH2 [K_{ss} (μmol l^{-1})]
Reference substrates		
APAL	2,560 ± 308	1,670 ± 115
ABAL	4,750 ± 1,074	1,840 ± 339
Synthetic substrates		
Ac-APAL	2,910 ± 485	1,520 ± 321
Propi-APAL	None	8,400 ± 1,425
Valer-APAL	21,700 ± 8,200	1,720 ± 511
3-Met-Butyr-APAL	None	4,620 ± 989
2,2-DiMet-Propi-APAL	6,510 ± 1,448	1,930 ± 692
Adip-APAL	3,450 ± 441	4,630 ± 936
Ac-ABAL	None	3,510 ± 742
Propi-ABAL	None	7,870 ± 1,293
2-Met-Propi-ABAL	8,140 ± 2,032	2,210 ± 541
3-Met-Butyr-ABAL	None	657 ± 157
2,2-diMet-Propi-ABAL	None	1,470 ± 298

The substrate inhibition constant values (K_{ss}) were determined with the GraphPad Prism 5.0 software using the formula $v = V_{max}\cdot[S]/(K_m + [S]\cdot(1 + [S]/K_{ss}))$ for nonlinear regression

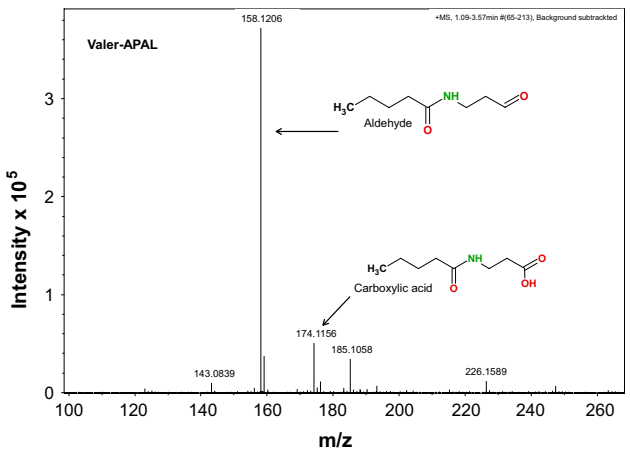

Fig. 4 MS analysis of product acid arising from Valer-APAL oxidation by PsAMADH1. The reaction mixture composed of 0.1 M ammonium bicarbonate buffer, pH 8.0, Valer-APAL (1.0 mM), NAD^+ (1.5 mM) and PsAMADH2 (21.8 μg·ml^{-1}) was kept at laboratory temperature with stirring overnight. Then the enzyme was removed by ultrafiltration and the filtrate diluted 10 fold prior to its injection to the mass spectrometer

Butyr-APAL and Butyr-ABAL were weaker substrates than the corresponding branched 2-Met-Propi derivatives. Similarly, Valer-APAL and Valer-ABAL were rather weaker substrates than their counterpart 3-Met-Butyr derivatives but they were better or at the same level of substrate properties like the 2-Met-Butyr derivatives (Table 2).

An excess substrate inhibition was observed roughly in one half of the measured saturation curves. The determined inhibition constants K_{ss} were between 0.65 and 21.7 mmol l^{-1} (Table 3). Five synthetic substrates, namely Ac-APAL, Valer-APAL, 2,2-diMet-Propi-APAL, 2-Met-Propi-ABAL and Adip-APAL inhibited both isoenzymes in excess concentrations. The respective substrate inhibition constants (K_{ss}) values were usually lower for PsAMADH2, which thus appears more prone to this mode of inhibition for the given set of compounds. In agreement with this finding, six other compounds (Propi-APAL, 3-Met-Butyr-APAL, Ac-ABAL, Propi-ABAL, 3-Met-Butyr-ABAL and 2,2-diMet-Propi-ABAL) inhibited in excess concentrations PsAMADH2 only. There was no substrate which would exclusively inhibit PsAMADH1 in this way. A stronger substrate inhibition (measured with natural substrates) was observed previously also for maize and tomato isoforms carrying Trp residue at the position equivalent to Trp288 in PsAMADH2 (Kopečný et al. 2013).

In order to confirm the formation of carboxylic acids as products of enzymatic conversion, selected *N*-acyl-ω-aminoaldehydes were subjected to reactions with PsAMADH1 (Valer-APAL and Propi-ABAL) or PsAMADH2 (2,2-diMet-Propi-APAL and 3-Met-Butyr-ABAL) in the presence of NAD^+. After a prolonged incubation, the reaction mixtures in a volatile buffer were diluted and analyzed by mass spectrometry for the presence of peaks with *m/z* values corresponding to the expected product acids. As an illustration, Fig. 4 shows a result obtained with Valer-APAL. In this case, the *N*-acyl aminoaldehyde was oxidized to 3-(valerylamino)propionic acid, which provided a signal with *m/z* 174.1 in the mass spectrum.

The kinetic results reported here demonstrate that plant ALDH10 enzymes oxidize various *N*-acyl-ω-aminoaldehydes including branched-chain structures. So far, no aldehyde compound with a branched carbon chain in the molecule has been studied in this regard. Substrate properties were much more affected by the number of carbon atoms of the core ω-aminoaldehyde chain than by the size and structural isomerism of the acyl substituent. It seems that plant ALDHs of this group could oxidize also other *N*-substituted derivatives of APAL and ABAL or aldehydes (including natural compounds) with structural features permitting similar orientation in the substrate channel and binding at the active site. It is worth of mentioning in this context that a conversion of 4-(3-aminopropylamino) butyraldehyde, which is the product of spermidine oxidation, has already been described (Šebela et al. 2000).

Docking experiments confirmed the affinity of PsAMADH2 to unbranched aliphatic *N*-acyl derivatives of APAL and ABAL as well as to 2,2-diMet-Propi- and

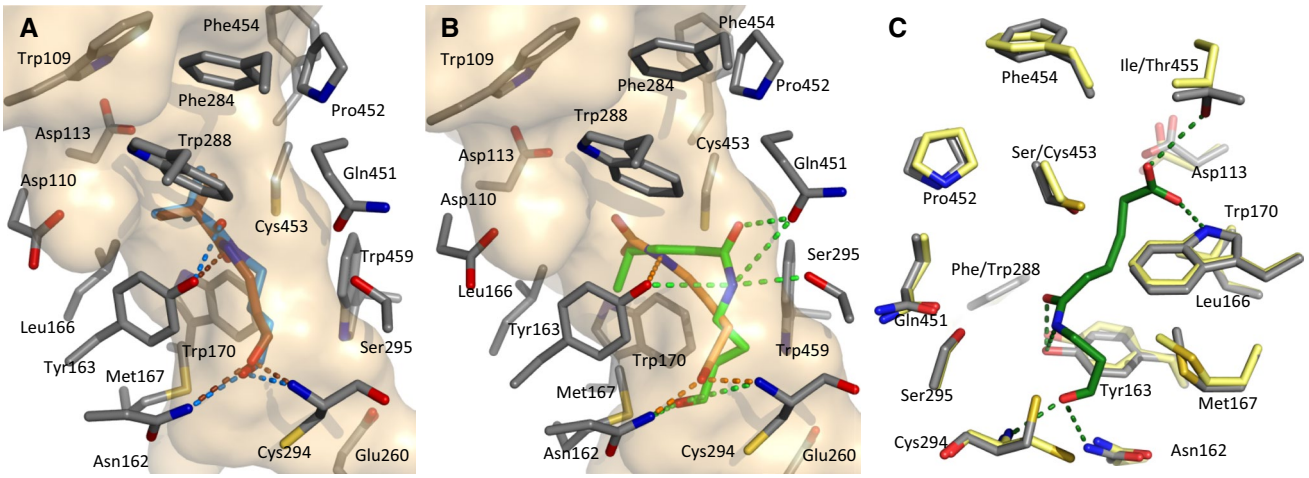

Fig. 5 Molecular docking of substrates into the active side of PsAMADH2, a general view. All residues lining the substrate channel and forming the active site are drawn in *grey*. The surface of the substrate channel is shown in *brownish yellow*. **a** Both tested *N*-(2,2-dimethylpropionyl) aminoaldehydes interact with the oxygen atom of Tyr163; 2,2-diMet-Propi-APAL (*brown*) binds via its nitrogen atom and 2,2-diMet-Propi-ABAL (*blue*) via its acyl oxygen atom. **b** Ac-ABAL (*orange*) interacts only with Tyr 163 via the nitrogen atom, whereas Valer-ABAL (*green*) shows an interaction with three residues—Tyr163, Ser295 and Gln451. **c** Adip-APAL interacts with Tyr163 via both nitrogen and oxygen atoms of its amide group. The carboxyl oxygen atoms of the ligand interact with the indole nitrogen atom of Trp170 and the hydroxyl oxygen atom of Thr455. In PsAMADH1 (its superposed active-site residues are shown here in *yellow*), Thr455 is replaced by Ile455. The aldehyde oxygen atom of the substrate is H-bonded to the side chains of Asn162 and the catalytic Cys294

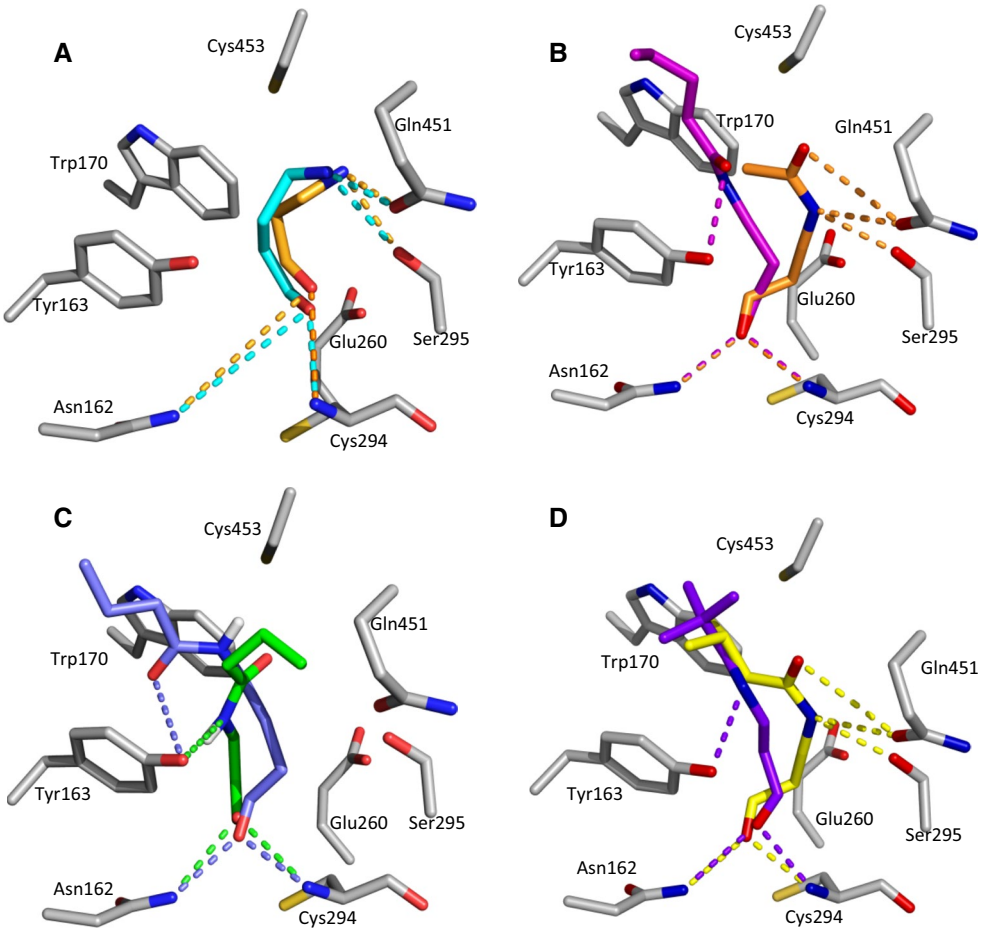

Fig. 6 Molecular docking of substrates into the active side of PsAMADH2, a detailed view. Active site residues of PsAMADH2 are drawn in *grey*. **a** The two physiological substrates APAL (*light orange*) and ABAL (*cyan blue*) interact with Ser295 and Gln451 via their amino group nitrogen atom. **b** While Ac-APAL (*orange*) probably interacts with Ser295 and Gln451, Valer-APAL (*purple*) interacts with Tyr163 via its acyl oxygen atom. **c** Both *N*-butyryl-ω-aminoaldehydes interact with Tyr 163, Butyr-APAL (*slate blue*) via its acyl oxygen atom and Butyr-ABAL (*green*) via its nitrogen atom. **d** 3-Met-Butyr-APAL (*yellow*) interacts with Ser295 and Gln451; on the other hand its isomer 2,2-diMet-Propi-APAL (*violet blue*) interacts with Tyr163. The aldehyde oxygen atom of the substrates establishes H-bond interactions with the side chains of Asn162 and the catalytic Cys294

Table 4 Possible interactions of substrate amide group atoms with substrate channel residues of PsAMADH2 and the respective docking energy values

Aldehyde	Energy		Possible interactions of substrate amide group atoms with substrate channel residues					
	Dock	Free	With Tyr163 OH		With Ser295 OG		With Gln451 OE1	
	(kcal/mol)	(kcal/mol)	Via N[a]	Via O[a]	Via N[a]	Via O[a]	Via N[a]	Via O[a]
APAL	−4.30	−3.62	–	–[b]	+	–[b]	+	–[b]
ABAL	−5.24	−4.20	–	–[b]	+	–[b]	+	–[b]
Ac-APAL	−5.60	−4.23	–	–	+	–	+	+
Propi-APAL	−5.43	−3.99	+	–	–	–	–	–
Butyr-APAL	−5.75	−3.83	+	–	–	–	–	–
Valer-APAL	−6.98	−4.60	–	+	–	–	–	–
3-Met-Butyr-APAL	−7.21	−5.15	–	–	+	–	+	+
2,2-DiMet-Propi-APAL	−6.38	−4.74	+	–	–	–	–	–
Adip-APAL	−7,73	−4,72	+	+	–	–	–	–
Ac-ABAL	−5.58	−3.93	+	–	–	–	–	–
Propi-ABAL	−6.03	−4.07	–	–	–	–	–	–
Butyr-ABAL	−7.10	−4.80	–	+	–	–	–	–
Valer-ABAL	−7.52	−5.08	+	–	+	–	+	+
3-Met-Butyr-ABAL	−7.56	−5.13	–	–	–	–	–	–
2,2-DiMet-Propi-ABAL	−7.19	−5.20	–	+	–	–	–	–

[a] Oxygen or nitrogen atom of the amide group of the substrate

[b] APAL and ABAL do not have a second oxygen atom, so there is no possibility of its interaction with substrate channel residues

3-Met-Butyr- derivatives (Figs. 5, 6). The respective values of free energy of binding and final docked energy are provided in Table 4 together with a list of interacting residues. There is no doubt that results of molecular docking of substrates into enzyme active sites have to be always interpreted carefully as this is just an approximation and obtaining crystal structures of the reacting molecules would provide data with higher confidence and biological value. The amide group of Ac-APAL was found to interact with OG atom of Ser295 and OE1 atom of Gln451; such an interaction was also demonstrated for the nitrogen atom of APAL amino group (Fig. 6). On the contrary, the amide group of longer *N*-acyl APAL derivates like Propi-APAL, Butyr-APAL and Valer-APAL did not provide any interaction with Ser295 and Gln451 but was in an H-bond distance from the side chain oxygen atom of Tyr163 (Fig. 6). Whereas Valer-APAL interacted with Tyr163 via the amide oxygen atom, both Propi-APAL, Butyr-APAL preferentially interacted via their amide nitrogen atom. ABAL was docked in a similar way like APAL. Conversely, the nitrogen atom of Ac-ABAL interacted with Tyr163 and not with Ser295 or Gln451. Butyr-ABAL was in a bond distance with Tyr163 via the acyl oxygen atom and Valer-ABAL interacted with Ser295 and Gln451 through both atoms from the amide group. Its nitrogen atom would then also interact with Tyr163. An interaction of 3-Met-Butyr-APAL with Ser295 via the substrate nitrogen atom and with Gln451 via both nitrogen and oxygen atom of the amide group was observed (Fig. 6). The two double branched substrates were found in an interaction with Tyr163: either through the nitrogen atom (2,2-diMet-Propi-APAL) or via the acyl oxygen (2,2-diMet-Propi-ABAL); Fig. 5.

The only substrate containing a carboxylic group—Adip-APAL—was added to this study in order to evaluate the ability of AMADHs to oxidize aldehydes with a negative charge in the molecule. Adip-APAL was among the weakest substrates of PsAMADH1 considering the V_{max}/K_m ratio. Unexpectedly, it was the best synthetic substrate for PsAMADH2 and it was even better substrate than naturally occurring ABAL. Docking experiments revealed that the terminal carboxyl group of Adip-APAL establishes an H-bond interaction with NE1 atom of Trp170 and OG1 atom of Thr455 while the amide group binds to Tyr163 of PsAMADH2. On the contrary, PsAMADH1 carries nonpolar Ile455 and cannot establish an H-bond to the carboxyl of Adip-APAL (Fig. 5). This fact probably leads to the huge difference between both isoenzymes in acceptance of Adip-APAL as a substrate.

The docking experiments revealed that the substrate properties of *N*-acyl-ω-aminoaldehydes arise from their proper binding at the active site, which is facilitated by interactions with amino acid residues in the substrate channel such as Tyr163. The previously suggested importance of Tyr163 in allowing substrates to enter the active site in a proper orientation, which was deduced from mutagenesis results (Kopečný et al. 2011), has now been confirmed.

Conclusions

Both isoenzymes of PsAMADH oxidized *N*-acyl derivatives of their natural substrates APAL and ABAL. Kinetic parameters of the oxidation were much more affected by the number of carbon atoms of the core ω-aminoaldehyde chain than by the size and structural isomerism of the acyl chain bound to the amino group. Generally, APAL derivatives were better substrates than the corresponding derivatives of ABAL. None of the synthetic compounds was more efficient than the best natural substrate APAL. Nevertheless, in the case of PsAMADH2, two synthetic substrates (Adip-APAL and Propi-APAL) were superior to the other natural aminoaldehydes ABAL and Ac-APAL. The enzymatic conversion was confirmed by LC–MS analysis of reaction products. Molecular docking indicated the possible interaction of the amide nitrogen and oxygen atoms of the synthetic substrates with three residues of PsAMADH2 substrate channel—Tyr163, Ser295 and Gln451. It becomes clear that ALDH10 enzymes may oxidize even more compounds than was expected. In addition to their known natural ω-aminoaldehyde and aldehyde substrates or the recently reported group of aromatic and heterocyclic aldehydes (Frömmel et al. 2012), the substrate specificity of plant ALDHs may also include certain acyl aldehydes or aldehydes with heteroatoms in their carbon chains (both linear or branched-chain structures) if they would bind properly at the active site, which is facilitated by interactions with substrate channel residues. This has a big implication for understanding the physiological role of plant ALDH10 enzymes, which might participate not only in polyamine metabolism and production of osmoprotectants but also in other metabolic pathways involving aldehydes (detoxification routes, secondary metabolism).

Acknowledgments This work was supported by Grant No. LO1204 from the Ministry of Education, Youth and Sports of the Czech Republic and Grant No. P501/11/1591 from the Czech Science Foundation. The authors thank for the access to computing and storage facilities owned by parties and projects contributing to the National Grid Infrastructure MetaCentrum provided under the program "Projects of Large Infrastructure for Research, Development, and Innovations" (LM2010005).

Conflict of interest The authors declare no conflict of interest.

References

Ando T, Yamawaki J (1979) Pottasium fluoride on celite. A versatile reagent for C-, N-, O- and S-alkylations. Chem Lett 1:45–46. doi:10.1246/cl.1979.45

Awal HMA, Yoshida I, Doe M, Hirasawa E (1995) 3-aminopropionaldehyde dehydrogenase of millet shoots. Phytochemistry 40:393–395. doi:10.1016/0031-9422(95)00293-G

Bradbury LMT, Gillies SA, Brushett DJ, Waters DLE, Henry RJ (2008) Inactivation of an aminoaldehyde dehydrogenase is responsible for fragnance in rice. Plant Mol Biol 68:439–449. doi:10.1007/s11103-008-9381-x

Brocker C, Vasiliou M, Carpenter S, Carpenter C, Zhang Y, Wang X, Kotchoni SO, Wood AJ, Kirch HH, Kopečný D, Nebert DW, Vasiliou V (2013) Aldehyde dehydrogenase (ALDH) superfamily in plants: gene nomenclature and comparative genomics. Planta 237:189–210. doi:10.1007/s00425-012-1749-0

Case DA, Cheatham III TE, Darden T, Gohlke H, Luo R, Merz Jr. KM, Onufriev A, Simmerling C, Wang B, Woods RJ (2005) The amber biomolecular simulation programs. J Comput Chem 26:1668–1688. doi:10.1002/jcc.20290

Chakraborty M, Karun A, Mitra A (2009) Accumulation of phenylpropanoid derivatives in chitosan-induced cell suspension culture of *Cocos nucifera*. J Plant Phys 166:63–71. doi:10.1016/j.jplph.2008.02.004

Díaz-Sánchez AG, González-Segura L, Mújica-Jiménez C, Rudiño-Piñera E, Montiel C, Martínez-Castilla LP, Muñoz-Clares RA (2012) Amino acid residues critical for the specificity for betaine aldehyde of the plant ALDH10 isoenzyme involved in the synthesis of glycine betaine. Plant Physiol 158:1570–1582. doi:10.1104/pp.112.194514

Frisch MJ, Trucks GW, Schlegel HB, Scuseria GE, Robb MA, Cheeseman JR, Montgomery JA Jr, Vreven T, Kudin KN, Burant JC, Millam JM, Iyengar SS, Tomasi J, Barone V, Mennucci B, Cossi M, Scalmani G, Rega N, Petersson GA, Nakatsuji H, Hada M, Ehara M, Toyota K, Fukuda R, Hasegawa J, Ishida M, Nakajima T, Honda Y, Kitao O, Nakai H, Klene M, Li X, Knox JE, Hratchian HP, Cross JB, Bakken V, Adamo C, Jaramillo J, Gomperts R, Stratmann RE, Yazyev O, Austin AJ, Cammi R, Pomelli C, Ochterski JW, Ayala PY, Morokuma K, Voth GA, Salvador P, Dannenberg JJ, Zakrzewski VG, Dapprich S, Daniels AD, Strain MC, Farkas O, Malick DK, Rabuck AD, Raghavachari K, Foresman JB, Ortiz JV, Cui Q, Baboul AG, Clifford S, Cioslowski J, Stefanov BB, Liu G, Liashenko A, Piskorz P, Komaromi I, Martin RL, Fox DJ, Keith T, Al-Laham MA, Peng CY, Nanayakkara A, Challacombe M, Gill PMW, Johnson B, Chen W, Wong MW, Gonzalez C, Pople JA (2004) Gaussian 03, Revision C.02. Gaussian Inc, Wallingford

Frömmel J, Soural M, Tylichová M, Kopečný D, Demo G, Wimmerová M, Šebela M (2012) Plant aminoaldehyde dehydrogenase oxidize a wide range of nitrogenous heterocyclic aldehydes. Amino Acids 43:1189–1202. doi:10.1007/s00726-011-1174-x

Fujiwara T, Hori K, Ozaki K, Yokota Y, Mitsuya S, Ichiyanagi T, Hattori T, Takabe T (2008) Enzymatic characterization of peroxisomal and cytosolic betaine aldehyde dehydrogenases in barley. Physiol Plant 134:22–30. doi:10.1111/j.1399-3054.2008.01122.x

Gaid MM, Sircar D, Beurle T, Mitra A, Beerhues L (2009) Benzaldehyde dehydrogenase from chitosan-treated *Sorbus aucuparia* cell cultures. J Plant Phys 166:1343–1349. doi:10.1016/j.jplph.2009.03.003

Hanson AD, Wyse R (1982) Biosynthesis, translocation, and accumulation of betaine in sugar beet and its progenitors in relation to salinity. Plant Physiol 70:1191–1198. doi:10.1104/pp.70.4.1191

Hanson AD, Rathinatasabapathi B, Rivoal J, Burnet M, Dillon MO, Gages DA (1994) Osmoprotective compounds in the Plumbaginaceae: a natural experiment in metabolic engineering of stress tolerance. Proc Natl Acad Sci USA 91:306–310. doi:10.1073/pnas.91.1.306

Kopečný D, Tylichová M, Snégaroff J, Popelková H, Šebela M (2011) Carboxylate and aromatic active-site residues are determinants of high-affinity binding of ω-aminoaldehydes to plant aminoaldehyde dehydrogenases. FEBS J 278:3130–3139. doi:10.1111/j.1742-4658.2011.08239.x

Kopečný D, Končitíková R, Tylichová M, Vigouroux A, Moskalíková H, Soural M, Šebela M, Moréra S (2013) Plant ALDH10 family: identifying critical residues for substrate specificity and trapping

a thiohemiacetal intermediate. J Biol Chem 288:9491–9507. doi:10.1074/jbc.M112.443952

Li W, Yuan XM, Ivanova S, Tracey KJ, Eaton JW, Brunk UT (2003) 3-Aminopropanal, formed during cerebral ischaemia, is a potent lysosomotropic neurotoxin. Biochem J 371:429–436. doi:10.1042/BJ20021520

Long MC, Nagegowda D, Kaminaga Y, Ho KK, Kish CM, Schnepp J, Sherman D, Weiner H, Rhodes D, Dudareva N (2009) Involvement of snapdragon benzaldehyde dehydrogenase in benzoic acid biosynthesis. Plant J 59:256–265. doi:10.1111/j.1365-313X.2009.03864.x

Matsuda H, Suzuki Y (1984) γ-Guanidinobutyraldehyde dehydrogenase of *Vicia faba* leaves. Plant Physiol 76:654–657. doi:10.1104/pp.76.3.654

Morris GM, Goodsell DS, Halliday RS, Huey R, Hart WE, Belew RK, Olson AJ (1998) Automated docking using a Lamarckian genetic algorithm and an empirical binding free energy function. J Comput Chem 19:1639–1662. doi:10.1002/(SICI)1096-987X(19981115)19:14<1639:AID-JCC10>3.0.CO;2-B

Pearlman DA, Case DA, Caldwell JW, Ross WS, Cheatham III TE, DeBolt S, Ferguson D, Seibel G, Kollman P (1995) Amber, a package of computer programs for applying molecular mechanics, normal mode analysis, molecular dynamics and free energy calculations to simulate the structural and energetic properties of molecules. Comput Phys Commun 91:1–41. doi:10.1016/0010-4655(95)00041-D

Peng X, Shindo K, Kanoh K, Inomata Y, Choi SK, Misawa N (2005) Characterization of *Sphingomonas* aldehyde dehydrogenase catalyzing the conversion of various aromatic aldehydes to their carboxylic acids. Appl Microbiol Biotechnol 69:141–150. doi:10.1007/s00253-005-1962-x

Prokop M, Adam J, Kříž Z, Wimmerová M, Koča J (2008) TRITON: a graphical tool for ligand-binding protein engineering. Bioinformatics 24:1955–1956. doi:10.1093/bioinformatics/btn344

Rhodes R, Rich PJ, Brunk DG, Ju GC, Rhodes JC, Pauly MH, Hansen LA (1989) Development of two isogenic sweet corn hybrids differing for glycinebetaine content. Plant Physiol 91:1112–1121. doi:10.1104/pp.91.3.1112

Rippa S, Zhao Y, Merlier F, Charrier A, Perrin Y (2012) The carnitine biosynthetic pathway in *Arabidopsis thaliana* shares similar features with the pathway of mammals and fungi. Plant Physiol Biochem 60:109–114. doi:10.1016/j.plaphy.2012.08.001

Schüttelkopf AW, van Aalten DMF (2004) PRODRG: a tool for high-throughput crystallography of protein-ligand complexes. Acta Cryst D60:1355–1363. doi:10.1107/S0907444904011679

Šebela M, Brauner F, Radová A, Jacobsen S, Havliš J, Galuszka P, Peč P (2000) Characterisation of a homogeneous plant aminoaldehyde dehydrogenase. Biochim Biophys Acta 1480:329–341. doi:10.1016/S0167-4838(00)00086-8

Shelp BJ, Bown AW, McLean MD (1999) Metabolism and functions of gamma-aminobutyric acid. Trends Plant Sci 4:446–452. doi:10.1016/S1360-1385(99)01486-7

Shelp BJ, Bozzo GG, Trobacher CP, Zarei A, Deyman KL, Brikis CJ (2012) Hypothesis/review: contribution of putrescine to 4-aminobutyrate (GABA) production in response to abiotic stress. Plant Sci 193:130–135. doi:10.1016/j.plantsci.2012.06.001

Smith PK, Krohn RI, Hermanson GT, Mallia AA, Gartner FH, Provenzano MD, Fujimoto EK, Goeke NM, Olson BJ, Klenk DC (1985) Measurement of protein using bicinchoninic acid. Anal Biochem 150:76–85. doi:10.1016/0003-2697(85)90442-7

Smith TA, Croker SJ, Loeffler RST (1986) Occurrence in higher-plants of 1-(3-aminopropyl)-pyrrolinium and pyrroline: products of polyamine oxidation. Phytochemistry 25:683–689. doi:10.1016/0031-9422(86)88024-4

Stiti N, Adewale IO, Petersen J, Bartels D, Kirch HH (2011) Engineering the nucleotide coenzyme specificity and sulfhydryl redox sensitivity of two stress-responsive aldehyde dehydrogenase isoenzymes of *Arabidopsis thaliana*. Biochem J 434:459–471. doi:10.1042/BJ20101337

Tavladoraki P, Rossi MN, Saccuti G, Perez-Amador MA, Polticelli F, Angelini R, Federico R (2006) Heterologous expression and biochemical characterization of a polyamine oxidase from *Arabidopsis* involved in polyamine back conversion. Plant Physiol 141:1519–1532. doi:10.1104/pp.106.080911

Trossat C, Rathinasabapathi B, Hanson AD (1997) Transgenically expressed betaine aldehyde dehydrogenase efficiently catalyzes oxidation of dimethylsulfoniopropionaldehyde and omega-aminoaldehydes. Plant Physiol 113:1457–1461. doi:10.1104/pp.113.4.1457

Tylichová M, Briozzo P, Kopečný D, Ferrero J, Moréra S, Joly N, Snégaroff J, Šebela M (2008) Purification, cystalization and preliminary crystalografic study of a recombinant plant aminoaldehyde dehydrogenace from *Pisum sativum*. Acta Cryst F64:88–90. doi:10.1107/S1744309107068522

Tylichová M, Kopečný D, Moréra S, Briozzo P, Lenobel R, Snégaroff J, Šebela M (2010) Structural and functional characterization of plant aminoaldehyde dehydrogenase from *Pisum sativum* with a broad specificity for natural and synthetic aminoaldehydes. J Mol Biol 396:870–882. doi:10.1016/j.jmb.2009.12.015

Vaz FM, Wanders RJA (2002) Carnitine biosynthesis in mammals. Biochem J 361:417–429. doi:10.1042/0264-6021:3610417

Weigel P, Weretilnyk EA, Hanson AD (1986) Betaine aldehyde oxidation by spinach chloroplasts. Plant Physiol 82:753–759. doi:10.1104/pp.82.3.753

Wood PL, Khan MA, Moskal JR (2007) The concept of "aldehyde load" in neurodegenerative mechanisms: cytotoxicity of the polyamine degradation products hydrogen peroxide, acrolein, 3-aminopropanal, 3-acetamidopropanal and 4-aminobutanal in a retinal ganglion cell line. Brain Res 1145:150–156. doi:10.1016/j.brainres.2006.10.004